A Platform for Large-Scale Graphene Electronics – CVD Growth of Single-Layer Graphene on CVD-Grown Hexagonal Boron Nitride

Min Wang, Sung Kyu Jang, Won-Jun Jang, Minwoo Kim, Seong-Yong Park, Sang-Woo Kim, Se-Jong Kahng, Jae-Young Choi, Rodney S. Ruoff, Young Jae Song, and Sungjoo Lee**

After graphene emerged as a material with the potential to supplant silicon in future electronic devices because of its superior electronic properties, there has been a flurry of investigations devoted to the development of high performance graphene-based electronic devices.[1] However, recent experimental and theoretical studies have shown that the substrate materials supporting graphene and the quality of the interface between graphene and the substrate have large impacts on the properties of graphene and device performance. The limitations of graphene-based devices, such as limited carrier mobility, Dirac point shift, and the hysteretic behavior of their *I*–*V* characteristics, result from trapped charges, surface roughness, charge carrier inhomogeneity, and surface optical phonons that are induced by the substrate materials, including the commonly used SiO_2.[2–8] For the quality of graphene-based devices to approach that of intrinsic graphene, a new approach is needed to the support of graphene that does not degrade its electrical properties. In an attempt to find a suitable substrate that does not exhibit electronic interlayer coupling with graphene, hexagonal boron nitride (h-BN) has recently received significant attention because its lattice parameters are similar to those of graphene; h-BN features 1.7% lattice mismatch with graphene, an atomically smooth surface, and strong ionic bonding in a planar hexagonal lattice structure, which result in the suppression of dangling bonds and surface charge traps. Indeed, scanning tunneling microscopy (STM) measurements have shown that exfoliated and CVD-grown graphene transferred onto exfoliated h-BN have electron-hole charge inhomogeneity that is two orders of magnitude lower than that on SiO_2.[9,10] Electron mobilities of up to 60 000 and 37 000 $cm^2\ V^{-1}\ s^{-1}$ for exfoliated and CVD-grown graphene transferred onto exfoliated h-BN, respectively, have been reported.[11,12] By transferring CVD-grown graphene onto CVD-grown h-BN, we have recently realized large-area graphene-based devices on h-BN with three-fold higher mobilities than those on SiO_2.[13] Graphene/h-BN structures obtained by transferring either mechanically exfoliated or CVD-grown graphene onto h-BN layers have shown device performance improvements,[11–14] and allowed for investigation of some aspects of fundamental physics of graphene on h-BN. However, it remains a challenge to completely prevent the adsorption of water molecules and other species into a large are a graphene/h-BN interface during the transfer process. Even more importantly, when a super lattice for a field-effect transistor is fabricated by sequential transfer of graphene and h-BN, the designed device performance is difficult to achieve with possible impurities in each interface and poor scalability.

In this work, we report the direct CVD growth of graphene onto CVD-grown h-BN film to obtain a pristine graphene/h-BN interface over a large area. A CVD-grown h-BN layer on Cu foil was used as the substrate; the experimental details of

Dr. M. Wang, S. K. Jang, Prof. S. Lee
SKKU Advanced Institute of Nanotechnology (SAINT)
Center for Human Interface Nanotechnology (HINT)
Samsung-SKKU Graphene Center
College of Information and Communication Engineering
Sungkyunkwan University (SKKU)
Suwon 440-746, Korea
E-mail: leesj@skku.edu

W.-J. Jang, Prof. S.-J. Kahng
Department of Physics
Korea University
Seoul 136-713, Korea

M. Kim, Prof. Y. J. Song
SKKU Advanced Institute of Nanotechnology (SAINT)
Center for Human Interface Nanotechnology (HINT)
Samsung-SKKU Graphene Center
Department of Physics
Sungkyunkwan University (SKKU)
Suwon 440-746, Korea
E-mail: yjsong@skku.edu

Dr. S.-Y. Park, Dr. J.-Y. Choi
Graphene Research Center
Samsung Advanced Institute of Technology
Yongin 446-712, Korea

Prof. S.-W. Kim
SKKU Advanced Institute of Nanotechnology (SAINT)
Center for Human Interface Nanotechnology (HINT)
Samsung-SKKU Graphene Center
School of Advanced Materials Science and Engineering
Sungkyunkwan University (SKKU)
Suwon 440-746, Korea

Prof. R. S. Ruoff
Department of Mechanical Engineering and the Materials Science and Engineering Program
The University of Texas at Austin
One University Station C2200, Austin, Texas 78712, USA

DOI: 10.1002/adma.201204904

the synthesis of CVD-grown h-BN on Cu can be found in our previous report.[13] A CVD growth of graphene on this h-BN film on Cu is then done (CVD growth conditions are described in the Supporting Information). Before it was transferred onto a SiO_2 substrate, sequentially grown CVD graphene/h-BN on Cu foil was studied with STM and scanning tunneling spectroscopy (STS), which show the almost ideal (i.e., unperturbed) electronic properties of graphene by the high crystallinity, epitaxy, and the clean interface achieved in this sequentially CVD-grown graphene/h-BN film. After transfer, transmission electron microscopy (TEM) and Raman spectroscopy confirmed that this structure is robust enough for a reliable transfer process. In addition, electrical transport measurements revealed that transistors based on this sequential CVD-grown graphene/h-BN film exhibit better electrical performance than those based on graphene mechanically transferred onto h-BN films or SiO_2 substrates. Transferring graphene onto dielectric substrates can thus be avoided by this direct growth method. The interface between graphene and h-BN, therefore, is also protected from external impurities during transfer of this hybrid structure onto any substrate. A direct growth of h-BN film on graphene was reported,[15] which can be combined with our method to make a new recipe to synthesize large area super lattice of graphene and h-BN.[16] As this direct growth of graphene on h-BN film is based on a CVD process, scalability can be readily achieved for industrial applications. Currently, the mechanism of direct CVD growth of graphene on h-BN film is not fully understood yet, and we're performing extended experiments of h-BN layer-dependent Cu-catalytic graphene growth with density functional theory (DFT) calculations in a separate work. This paper, therefore, is focused on the successful direct CVD growth of graphene on h-BN film, and its superior electronic properties.

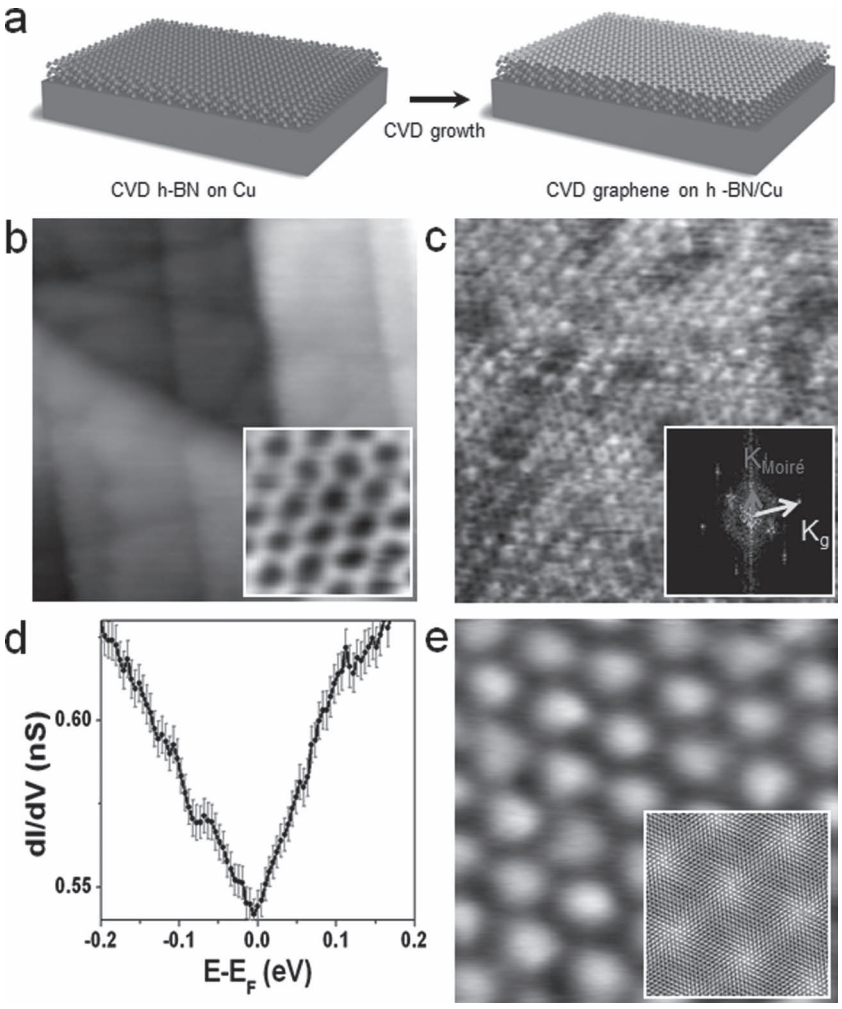

Figure 1. STM/STS data measured in a graphene layer on BN/Cu-foil. a) Schematic of graphene directly grown on CVD h-BN film/Cu foil for STM measurements. b) A large-scale STM image with the straight step edges of the underlying h-BN layers. Image area: 60 nm × 60 nm; parameters: V_b = 1.0 V, I_t = 0.1 nA. Inset) An STM image of the graphene honeycomb lattice. c) An STM image showing the Moiré pattern with a 0.55 nm period. Inset) The FFT result of (c). Image area: 10 nm × 10 nm; parameters: V_b = –0.8 V, I_t = 0.12 nA. d) Averaged dI/dV spectrum data measured on the region of 0.55 nm Moiré pattern with the error bars overlaid at each energy point; parameters: V_b = 0.2 V, I_t = 0.2 nA. e) An STM image showing the Moiré pattern of 4.2 nm period. Image area: 23 nm × 23 nm. Parameters: V_b = –0.14 V, I_t = 0.11 nA. Inset) A simulated Moiré pattern (4.2 nm) with an angle of 3.2° between the graphene and the h-BN.

We performed STM and STS measurements to reveal the atomic and electronic structures of graphene directly grown on CVD h-BN film on Cu foil as described in **Figure 1**a. As the CVD-grown h-BN layers are covered with a single-layer of graphene, the features in the large-scale image (60 nm × 60 nm) in Figure 1b are due to the underlying h-BN layers. Even though the h-BN layers were grown on polycrystalline Cu foil, they contain atomically flat terraces often with angles of 60°, 120°, or that are parallel between two step edges.[13] In this region, an atomic resolution STM image clearly shows the honeycomb lattice of graphene as shown in the inset of Figure 1b. Because h-BN has the similar atomic structures with graphene, we observed hexagonal Moiré patterns. In most cases, a period of 0.55 nm is observed as shown in Figure 1c. Considering the 1.7% lattice mismatch between graphene and h-BN, the periods of the Moiré patterns are determined by the rotational stacking angle between graphene and the underlying h-BN layers. We measured the angles between the Moiré patterns and the graphene lattices as well as their periods and found that the stacking angles between graphene and the h-BN layers are 26.0° for the 0.55 nm Moiré pattern.[17] An important feature of the graphene/h-BN hybrid structure is that the electronic states of graphene supported by the inert and flat h-BN layers are close to that of intrinsic graphene.[9,18,19] Figure 1d shows an averaged dI/dV spectrum obtained from the STS measurements for the 0.55 nm Moiré pattern region;

error bars are overlaid at each energy point. The overall spectrum has a sharp and symmetric V-shape with the Dirac point at the Fermi level, which is, to the best of our knowledge, the closest to that of intrinsic graphene yet reported. The statistics of the STS spectra indicate that the CVD-grown graphene in this structure is charge neutral and unperturbed by the CVD-grown h-BN substrate. This result, therefore, implies that there is essentially no charge transfer or doping from the underlying h-BN without metal or other impurities at the graphene/h-BN interface. The narrow width of the error bars at each energy point over a large area also indicates that this graphene on h-BN has the unperturbed and uniform electronic structure of Dirac fermions on a large scale. In some regions, Moiré patterns with different periods were observed. For example, the STM image in Figure 1e shows a Moiré pattern with a 4.2 nm period, and the angle between graphene and BN lattices is estimated to be 3.2°. The inset in Figure 1e is a simulated STM image, which shows a good agreement with the experimental data. As revealed by STM images and STS spectra measured on the graphene/h-BN film/Cu foil, the observed honeycomb lattice, Moiré patterns, and sharp and symmetric V-shape spectrum with the Dirac point at the Fermi level, show that high quality single-layer graphene was grown on the h-BN films on Cu without charge transfer or doping effects.

The microstructure, thickness, and robustness of the CVD-grown graphene/CVD-grown h-BN films were characterized by cross-sectional TEM before and after transferring the graphene/h-BN film onto a SiO_2/Si substrate. **Figure 2**a shows the cross-sectional TEM image of the Pt–graphene/h-BN–Cu foil interfaces before transferring, which confirms the presence of a graphene/h-BN film; the film thickness is approximately 2 nm. This film was transferred onto a SiO_2/Si substrate, whose cross-sectional TEM image (Figure 2b) also shows the layered structure of graphene/h-BN. Combined with our atomic resolution STM measurements on the top surface, cross-sectional TEM measurements before/after transfer show that the as-grown graphene/h-BN film is well crystallized and also robust enough to survive during the transfer process. Electron energy loss spectroscopy (EELS) was used for elemental analysis of the films to determine their chemical composition. Figure 2c shows an EELS spectrum with three visible edges starting at around 200, 290, and 410 eV, which correspond to the characteristic K-shell ionization edges of B, C, and N, respectively; the inset is the top view TEM image of the graphene/h-BN film where the EELS spectrum was obtained from.

To confirm that h-BN film is still remaining even after CVD growth of graphene, UV–vis absorption measurements were conducted. The observed absorption peak at 200 nm of h-BN film corresponds to its optical band gap,[20] the peak around 270 nm of graphene originates from π plasmon peak,[21] and thus the simultaneously appeared two peaks in the as-grown graphene/h-BN sample clearly show the coexistence of graphene and h-BN, as shown in Figure 2d. These results reveal strong evidence that h-BN can survive in the sequential CVD growth of graphene. Figure 2f shows selected-area electron diffraction (SAED) data of graphene/h-BN in the marked area in Figure 2e. This data demonstrates two sets of hexagonal diffraction patterns in our graphene/h-BN sample, providing a strong evidence of the coexistence of single crystal graphene and h-BN. Furthermore, this graphene/h-BN seems to have a preferential

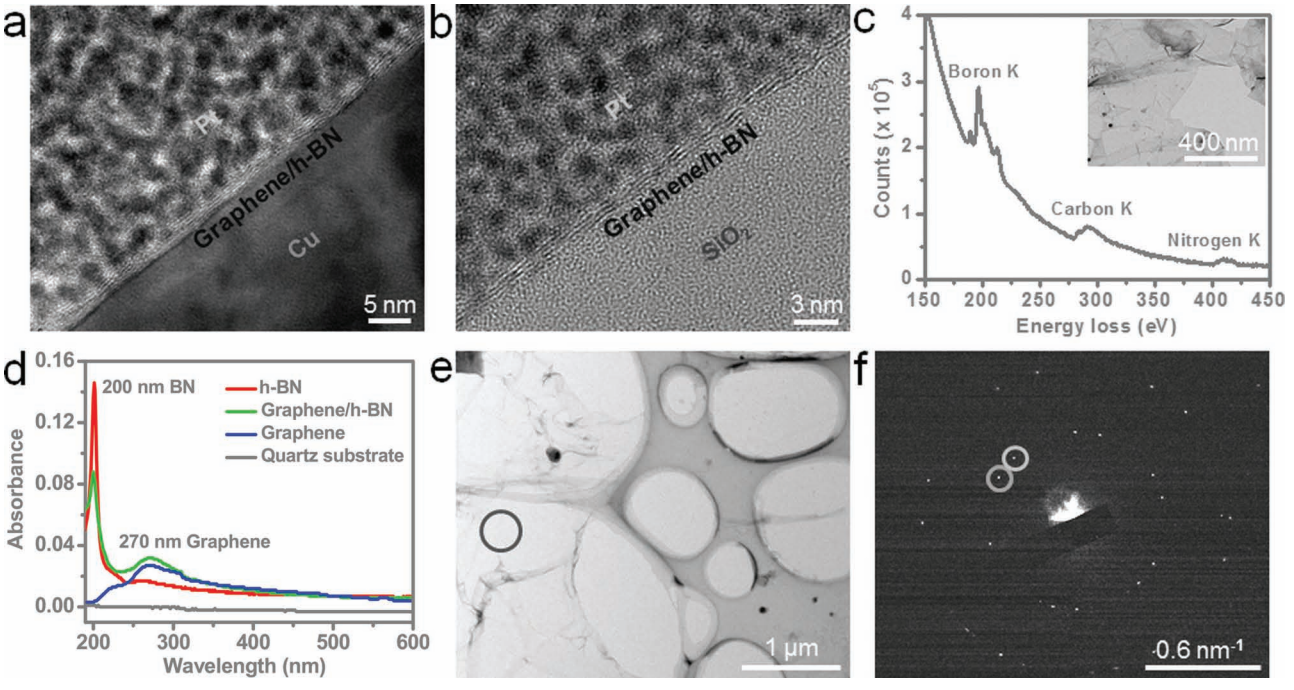

Figure 2. Cross-sectional TEM images of: a) a CVD-grown graphene/h-BN film on Cu foil; b) a CVD-grown graphene/h-BN film transferred onto a SiO_2/Si substrate. c) EELS spectrum showing the elements B, N, and C. Inset) Top-view TEM image of graphene/h-BN film. d) UV–vis absorption curve of CVD-grown h-BN, graphene/h-BN and graphene. e) Low-magnification TEM image of a graphene/h-BN film. f) Selected-area electron diffraction (SAED) data of graphene/h-BN in the marked area in (e).

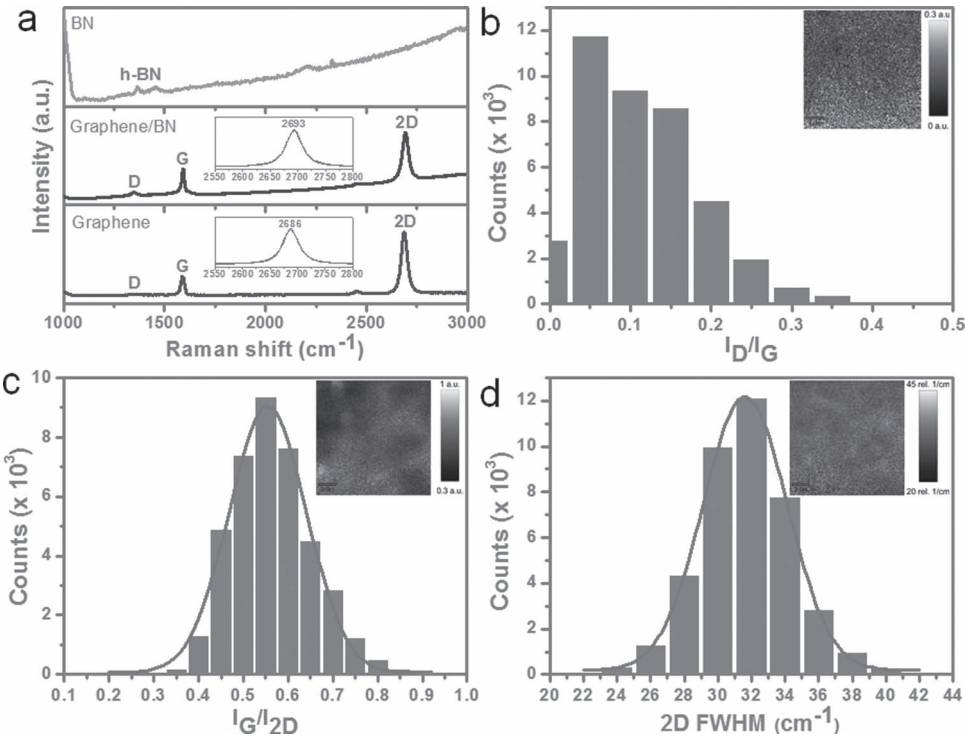

Figure 3. a) Typical 532 nm laser excited Raman spectra of h-BN, CVD-grown graphene/h-BN, and graphene transferred onto SiO_2/Si substrates. The insets shows a comparison of the 2D bands of the graphene/h-BN structure (above) and the graphene film (below). Statistical histograms for: b) I_D/I_G ratio, c) I_G/I_{2D} ratio, and d) 2D band FWHM of the CVD-grown graphene/h-BN film for an area of 20 μm^2. Inset) The corresponding Raman mapping images; scale bars: 3 μm.

stacking order within the size of SAED measurements, but we need to study more about this issue carefully.

While the quality of graphene/h-BN film was assessed at atomic scale by STM/STS and TEM measurements, Raman spectra were acquired for the graphene/h-BN film transferred onto the SiO_2/Si substrate to evaluate the quality, thickness, and uniformity at a larger length scale. Without a graphene layer on the h-BN film, the Raman spectrum in **Figure 3**a shows one dominant peak at 1368 cm^{-1} due to the E_{2g} vibrational mode of h-BN.[13] After CVD graphene growth, the visible characteristic peaks of graphene G and 2D bands at 1593 and 2693 cm^{-1}, respectively, show that graphene was grown on CVD-grown h-BN. The G and 2D bands of our CVD graphene are located at 1587 and 2686 cm^{-1}, and the reported G and 2D bands of mechanically exfoliated graphene are at 1582 and 2700 cm^{-1}.[22] This slight shift of G and 2D peak positions in a graphene/h-BN hybrid structure is probably due to the biaxial strain or other form of strain caused between graphene and underlying h-BN film.[23–27] The peak at 1345 cm^{-1} might be due to the superposition of the E_{2g} mode of the B-N vibration and the D band of graphene. The Raman spectra of CVD-grown graphene/CVD-grown h-BN and graphene contain a narrow and symmetric Lorentzian 2D peak (see the inset in Figure 3a) with a full width at half-maximum (FWHM) of approximately 34 cm^{-1} and a peak intensity ratio $I_G/I_{2D} < 0.5$, which are characteristic of single-layer graphene.[22] The statistical histogram based on the Raman mapping in Figure 3b shows that ≈93% of the graphene film grown on h-BN exhibits a peak intensity ratio $I_D/I_G < 0.2$, which is much smaller than that of few-layer graphene grown on h-BN powders and h-BN/Al_2O_3,[28,29] and is even comparable with those of graphene grown on Cu and Ni.[30–32] The I_G/I_{2D} ratio in Figure 3c falls into the range 0.2–0.9 with 84% in the range 0.45–0.65. These values are much smaller than the representative value (≈1) for bilayer graphene.[30,32–34] The 2D band FWHM (Figure 3d) is in the range of 24–40 cm^{-1} with 92% in the range of 28–36 cm^{-1}, which is much smaller than the 2D band FWHM (45–60 cm^{-1}) of bilayer graphene.[33,34] These results demonstrate that high-quality single-layer graphene was successfully grown in large scale on the CVD-grown h-BN film by direct CVD growth.

Electrical transport measurements were then performed to demonstrate the improvement in the quality of a graphene-based device obtained as a result of growing graphene directly onto CVD-grown h-BN. After the transfer of the samples onto a SiO_2/Si substrate, field-effect transistors with 5 μm channel length and 5 μm width were fabricated; the heavily doped Si substrate acts as a back gate that modulates the charge density in the graphene. The metallic source/drain electrodes were defined by photolithography followed by Au/Cr (50/5 nm) evaporation and a lift-off process. **Figure 4**a describes three different graphene systems; (blue) CVD-graphene transferred directly onto a SiO_2/Si substrate, (green) CVD-graphene transferred onto h-BN flakes, and (red) graphene directly grown on a CVD-h-BN film. All the color schemes correspond to those in each spectrum in Figure 4. Figure 4b shows the device resistance as a function of the applied back gate voltage Vg for the transistors

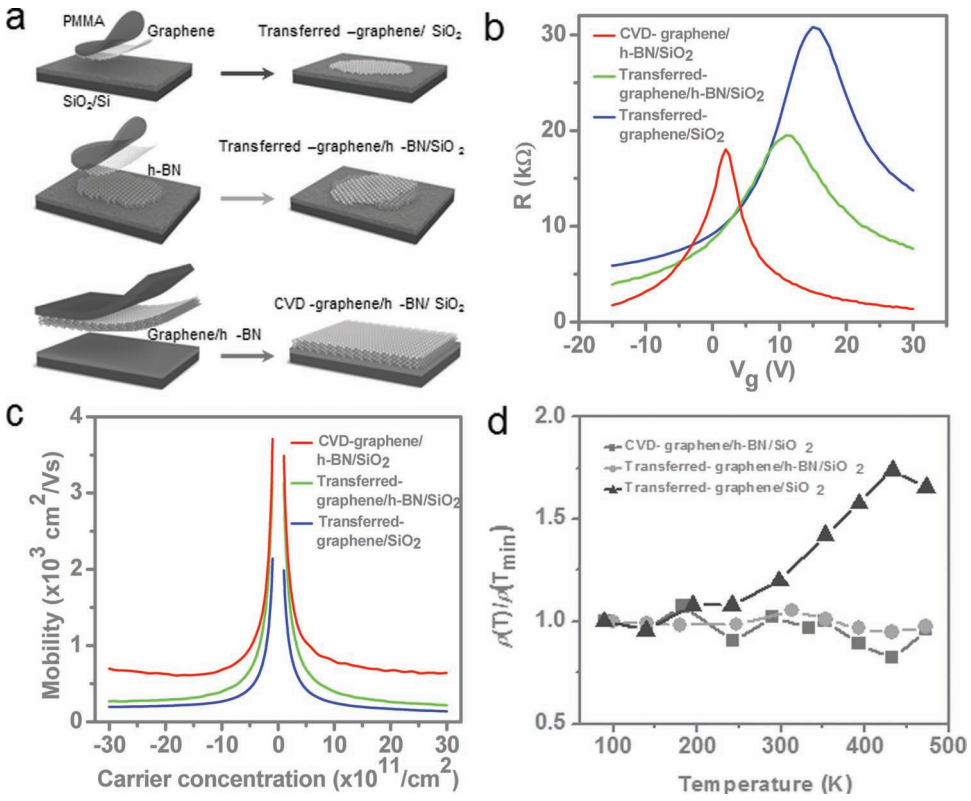

Figure 4. a) Scheme of three different graphene system; (blue) graphene transferred onto a SiO_2/Si substrate, (green) CVD-graphene transferred onto h-BN/SiO_2, and (red) large area CVD-graphene directly grown on CVD-grown h-BN film. b) Resistance versus applied gate voltage for CVD-grown graphene/h-BN, mechanically transferred graphene/h-BN, and graphene on SiO_2. c) Carrier mobility as a function of charge carrier density for the three devices. d) Temperature dependences of the resistivity at $V_g - V_{Dirac} = 10$ V for the three devices.

fabricated with CVD-grown graphene/h-BN (red), mechanically transferred graphene/h-BN (green), and graphene only (blue), all transferred onto the 90 nm SiO_2/Si substrate. The resistance curves have a largely symmetric shape around $V_g = V_{Dirac}$ and each passes through a maximum at this voltage, where V_{Dirac} = 1, 11, and 15 V for the CVD-grown graphene/h-BN, the mechanically transferred graphene/h-BN, and the graphene only devices, respectively. A nonzero value of V_{Dirac} indicates the presence of unintentional doping in graphene devices,[35] which could originate from charged impurities. A smaller value of V_{Dirac} indicates lighter doping and fewer charged impurities in the CVD-grown graphene/h-BN film. The charge-carrier inhomogeneity resulting from electron-hole puddle formation at low carrier densities can be estimated from the minimum conductivity plateau at the Dirac point.[36] Figure 4b shows that the CVD-grown graphene/h-BN device has a narrower minimum conductivity plateau, which implies the suppression of the charge-carrier inhomogeneity through the reduction in the number of charged impurities. This result shows that some charged impurities are present in the mechanically transferred graphene/h-BN interface, that is, residues and adsorbates arising during the transfer process, which can be limited and even eliminated through the direct CVD growth of graphene on h-BN. Theoretical and experimental studies have shown that the minimum conductivity at the Dirac point depends strongly on the number of charged impurities.[37,38] The minimum conductivities of the CVD-grown graphene/h-BN and the mechanically transferred graphene/h-BN are higher than that of graphene/SiO_2, which indicates that the use of the h-BN substrate enables a reduction in the charged impurity in the graphene/dielectric interface. Figure 4c shows the carrier mobility, which was determined by applying the Drude model,[13] as a function of the carrier density n, induced by $n = C_g(V_g - V_{Dirac})/e$, using the gate capacitance C_g obtained from geometrical considerations. For devices with CVD-grown graphene/h-BN fabricated on the SiO_2 substrate, an increase by a factor of approximately 2–3 in the carrier mobility was obtained over those of the mechanically transferred graphene/h-BN/SiO_2 and the graphene/SiO_2 devices in the range $n \approx 10^{11}$–10^{12} cm^2. Carrier transport in graphene transistors at low carrier densities is known to be predominantly determined by long-range Coulomb scattering with a short mean free path of ≈50 nm compared with that of the long mean free path of ≈1 μm for short-range scattering.[38] The observed higher carrier mobility of the CVD-grown graphene/h-BN devices in the low carrier density regime can, therefore, be attributed to the suppression of charged impurities. The temperature dependences of the resistivity at high densities ($V_g - V_{Dirac} = 10$ V) for the three samples are shown in Figure 4d. The resistivities of the CVD-grown graphene/h-BN and the mechanically transferred graphene/h-BN, show weak temperature dependence. For the graphene on SiO_2, the temperature dependence is linear at low

temperatures, and becomes highly non-linear at high temperatures; the critical temperature is approximately 220 K. These findings agree with the results of previous studies.[4,11] Two distinct contributions to the scattering in graphene on SiO_2 were found: by acoustic phonons in graphene and by remote interfacial phonons at the graphene-SiO_2 interface, which are likely to be due to charge impurities in the SiO_2 substrate.[39] These results show that no activated remote surface phonons were observed for the CVD-grown graphene/h-BN devices up to room temperature.

In conclusion, we have reported a new method for the synthesis and fabrication of a graphene/h-BN hybrid structure retaining a clean graphene/h-BN interface by using sequential CVD growth of single-layer graphene directly onto a CVD-grown h-BN film on Cu. The crystallinity, epitaxy, and electronic structures of the graphene/h-BN film and its interface states were assessed by atomic scale STM/STS measurements. Cross-sectional TEM measurements showed that the CVD-grown graphene/h-BN films are robust enough to survive during the transfer onto other substrates. Raman spectra and SAED confirmed large-scale uniform single-layer graphene directly grown on the h-BN film. Electrical carrier-transport measurements demonstrated that the CVD-grown graphene/h-BN devices exhibited superior carrier mobility and suppression of charged impurities, compared to those based on mechanically transferred graphene onto h-BN film or SiO_2 substrate. Our work demonstrates the capability of large-area growth of graphene/h-BN hybrid structure with an impurity free interface demanded for graphene-based devices.

Experimental Section

Synthesis: To grow graphene on h-BN, a CVD-grown h-BN layer on Cu foil was used as the substrate; the experimental details of the synthesis of CVD-grown h-BN on Cu can be found in our previous report.[13] We grew graphene on h-BN/Cu at 1000 °C for 40 min with 5 sccm H_2 and 20 sccm CH_4 for 40 min at a total pressure of 210 mTorr. After growth, the CVD-grown graphene/h-BN films were transferred onto target substrates using an ammonium persulfate aqueous solution. The growth and transfer details can be seen in the Supporting Information.

Characterization: STM/STS measurements with a Pt/Ir tip were performed on graphene/h-BN/Cu-foil at a temperature of 80 K and with a pressure of $\approx 5.0 \times 10^{-11}$ Torr. The typical thickness of the h-BN films is approximately 2 nm, so Cr/Au electrodes were deposited onto the graphene surface with shadow mask to apply a sample bias voltage to the graphene. The cross-sectional structures were prepared by using the lift out technique in focus ion beam (FIB) and studied by TEM (FEI Titan) under an acceleration voltage of 300 kV. UV–vis absorption (UV-3600) was conducted on the samples after transfer onto quartz substrate. Raman spectroscopy was performed on the samples after transfer onto 90 nm SiO_2/Si with a laser micro-Raman spectrometer (Kaiser Optical System Model RXN 532-nm excitation wavelength). Electronic-transport results were acquired under vacuum (from 1.7×10^{-6} Torr at 473 K to 6.6×10^{-8} Torr at 88 K, with the XYZ system).

Supporting Information

Supporting Information is available from the Wiley Online Library or from the author.

Acknowledgements

This research was supported by the Basic Science Research Program through the National Research Foundation of Korea (NRF) funded by the Ministry of Education, Science and Technology (Grant Numbers: 2009-0083540, 2012R1A1A2020089, and 2012R1A1A1041416). This work was supported by the Postdoctoral Research Program of Sungkyunkwan University (2012).

Received: November 29, 2012
Revised: January 24, 2013
Published online: April 10, 2013

[1] A. K. Geim, K. S. Novoselov, *Nat. Mater.* **2007**, *6*, 183.
[2] Y. B. Zhang, V. W. Brar, C. Girit, A. Zettl, M. F. Crommie, *Nat. Phys.* **2009**, *5*, 722.
[3] T. Ando, *J. Phys. Soc. Jpn.* **2006**, *75*, 074716.
[4] J. H. Chen, C. Jang, S. D. Xiao, M. Ishigami, M. S. Fuhrer, *Nat. Nanotechnol.* **2008**, *3*, 206.
[5] J. Martin, N. Akerman, G. Ulbricht, T. Lohmann, J. H. Smet, K. Von Klitzing, A. Yacoby, *Nat. Phys.* **2008**, *4*, 144.
[6] M. Lafkioti, B. Krauss, T. Lohmann, U. Zschieschang, H. Klauk, K. von Klitzing, J. H. Smet, *Nano Lett.* **2010**, *10*, 1149.
[7] H. M. Wang, Y. H. Wu, C. X. Cong, J. Z. Shang, T. Yu, *ACSNano* **2010**, *4*, 7221.
[8] Y. G. Lee, C. G. Kang, U. J. Jung, J. J. Kim, H. J. Hwang, H. J. Chung, S. Seo, R. Choi, B. H. Lee, *Appl. Phys. Lett.* **2011**, *98*, 183508.
[9] J. M. Xue, J. Sanchez-Yamagishi, D. Bulmash, P. Jacquod, A. Deshpande, K. Watanabe, T. Taniguchi, P. Jarillo-Herrero, B. J. Leroy, *Nat. Mater.* **2011**, *10*, 282.
[10] R. Decker, Y. Wang, V. W. Brar, W. Regan, H. Z. Tsai, Q. Wu, W. Gannett, A. Zettl, M. F. Crommie, *Nano Lett.* **2011**, *11*, 2291.
[11] C. R. Dean, A. F. Young, I. Meric, C. Lee, L. Wang, S. Sorgenfrei, K. Watanabe, T. Taniguchi, P. Kim, K. L. Shepard, J. Hone, *Nat. Nanotechnol.* **2010**, *5*, 722.
[12] W. Gannett, W. Regan, K. Watanabe, T. Taniguchi, M. F. Crommie, A. Zettl, *Appl. Phys. Lett.* **2011**, *98*, 242105.
[13] K. H. Lee, H. J. Shin, J. Lee, I. Y. Lee, G. H. Kim, J. Y. Choi, S. W. Kim, *Nano Lett.* **2012**, *12*, 714.
[14] P. J. Zomer, S. P. Dash, N. Tombros, B. J. van Wees, *Appl. Phys. Lett.* **2011**, *99*, 232104.
[15] Z. Liu, L. Song, S. Z. Zhao, J. Q. Huang, L. L. Ma, J. N. Zhang, J. Lou, P. M. Ajayan, *Nano Lett.* **2011**, *11*, 2032.
[16] L. Britnell, R. V. Gorbachev, R. Jalil, B. D. Belle, F. Schedin, A. Mishchenko, T. Georgiou, M. I. Katsnelson, L. Eaves, S. V. Morozov, N. M. R. Peres, J. Leist, A. K. Geim, K. S. Novoselov, L. A. Ponomarenko, *Science* **2012**, *335*, 947.
[17] M. Yankowitz, J. M. Xue, D. Cormode, J. D. Sanchez-Yamagishi, K. Watanabe, T. Taniguchi, P. Jarillo-Herrero, P. Jacquod, B. J. LeRoy, *Nat. Phys.* **2012**, *8*, 382.
[18] Y. J. Song, A. F. Otte, Y. Kuk, Y. K. Hu, D. B. Torrance, P. N. First, W. A. de Heer, H. K. Min, S. Adam, M. D. Stiles, A. H. MacDonald, J. A. Stroscio, *Nature* **2010**, *467*, 185.
[19] D. L. Miller, K. D. Kubista, G. M. Rutter, M. Ruan, W. A. de Heer, P. N. First, J. A. Stroscio, *Science* **2009**, *324*, 924.
[20] K. K. Kim, A. Hsu, X. T. Jia, S. M. Kim, Y. S. Shi, M. Hofmann, D. Nezich, J. F. Rodriguez-Nieva, M. Dresselhaus, T. Palacios, J. Kong, *Nano Lett.* **2012**, *12*, 161.
[21] R. R. Nair, P. Blake, A. N. Grigorenko, K. S. Novoselov, T. J. Booth, T. Stauber, N. M. R. Peres, A. K. Geim, *Science* **2008**, *320*, 1308.
[22] L. M. Malard, M. A. Pimenta, G. Dresselhaus, M. S. Dresselhaus, *Phys. Rep.* **2009**, *473*, 51.
[23] Z. H. Ni, H. M. Wang, Y. Ma, J. Kasim, Y. H. Wu, Z. X. Shen, *ACS Nano* **2008**, *2*, 1033.

[24] T. Yu, Z. H. Ni, C. L. Du, Y. M. You, Y. Y. Wang, Z. X. Shen, *J. Phys. Chem. C.* **2008**, *112*, 12602.
[25] M. Y. Huang, H. G. Yan, C. Y. Chen, D. H. Song, T. F. Heinz, J. Hone, *Proc. Natl. Acad. Sci. USA* **2009**, *106*, 7304.
[26] F. Ding, H. X. Ji, Y. H. Chen, A. Herklotz, K. Dorr, Y. F. Mei, A. Rastelli, O. G. Schmidt, *Nano Lett.* **2010**, *10*, 3453.
[27] C. Metzger, S. Remi, M. K. Liu, S. V. Kusminskiy, A. H. C. Neto, A. K. Swan, B. B. Goldberg, *Nano Lett.* **2010**, *10*, 6.
[28] T. Q. Lin, Y. M. Wang, H. Bi, D. Y. Wan, F. Q. Huang, X. M. Xie, M. H. Jiang, *J. Mater. Chem.* **2012**, *22*, 2859.
[29] K. Kim, J. Y. Choi, T. Kim, S. H. Cho, H. J. Chung, *Nature* **2011**, *479*, 338.
[30] Z. Z. Sun, Z. Yan, J. Yao, E. Beitler, Y. Zhu, J. M. Tour, *Nature* **2010**, *468*, 549.
[31] Y. J. Ren, C. F. Zhu, W. W. Cai, H. F. Li, Y. F. Hao, Y. P. Wu, S. S. Chen, Q. Z. Wu, R. D. Piner, R. S. Ruoff, *Nano* **2012**, *7*, 1150001.
[32] A. Reina, X. T. Jia, J. Ho, D. Nezich, H. B. Son, V. Bulovic, M. S. Dresselhaus, J. Kong, *Nano Lett.* **2009**, *9*, 30.
[33] S. S. Chen, W. W. Cai, R. D. Piner, J. W. Suk, Y. P. Wu, Y. J. Ren, J. Y. Kang, R. S. Ruoff, *Nano Lett.* **2011**, *11*, 3519.
[34] S. Lee, K. Lee, Z. H. Zhong, *Nano Lett.* **2010**, *10*, 4702.
[35] E. H. Hwang, S. Adam, S. Das Sarma, *Phys. Rev. Lett.* **2007**, *98*, 186806.
[36] K. I. Bolotin, K. J. Sikes, Z. Jiang, M. Klima, G. Fudenberg, J. Hone, P. Kim, H. L. Stormer, *Solid State Commun.* **2008**, *146*, 351.
[37] S. Adam, E. H. Hwang, V. M. Galitski, S. Das Sarma, *Proc. Natl. Acad. Sci. USA* **2007**, *104*, 18392.
[38] Y. W. Tan, Y. Zhang, K. Bolotin, Y. Zhao, S. Adam, E. H. Hwang, S. Das Sarma, H. L. Stormer, P. Kim, *Phys. Rev. Lett.* **2007**, *99*, 246803.
[39] J. Schiefele, F. Sols, F. Guinea, *Phys. Rev. B* **2012**, *85*, 195420.